Multi-Objective Optimization of Microstructures Embedded in MCHS for Enhancing Thermal Management of Electronic Components

Mosab Sakkay[1*], *Ihssane* El Ghandouri[1], *Anass* El Maakoul[2], *Said* Saadeddine[1], and *Mohamed* Meziane[3]

[1]Thermofluids and Numerical Simulation, MSPASI Lab, Faculty of Sciences and Techniques, UH2C, Casablanca, Morocco
[2]LERMA Lab, International University of Rabat, 11 100, Sala Al Jadida, Morocco
[3]Laboratory of Materials, Energy and Control Systems, Faculty of Sciences and Techniques, UH2C, Casablanca, Morocco

Abstract. Microelectronics dissipate more heat as their performance and functionality improve. MCHS has been considered one of the prominent techniques for the cooling of microelectronic components, where higher heat removal can be achieved by integrating microstructures into MCHS and optimizing channel geometry. A novel configuration of microstructures in a horizontal cylindrical shape integrated in different patterns has been extensively investigated to compare the thermohydraulic and thermodynamic performance of conventional vertical micro-pillars and novel horizontal micro-pillars. Numerical study has been carried out employing commercial CFD code "ANSYS Fluent" for the simulation of the different configurations of horizontal micro-pillars and vertical micro-pillars for Reynolds numbers spanning from 300 to 740. Fluid flow characteristics and temperature field distribution have been examined to understand the effect of flow behaviour on the cooling performance of microchannels. Alternating horizontal micro-pillars and vertical micro-pillars results in a comprehensive high cooling performance where both normalwise secondary flow and spanwise secondary flow are obtained. Multi-objective optimization has been employed to provide optimal micro-pillar dimensions and patterns. Increased temperature uniformity and enhanced entropy generation are obtained through the integration of the novel configuration of horizontal micro-pillars into MCHS.

1 Introduction

Since 1980s, when Tuckerman and Pease [1] first introduced heat sinks with parallel channels with micro dimensions, the MCHS has been the focus of researchers to improve heat removal from microelectronic devices. Downsizing electronic components necessitates adequate cooling to deal with the high heat flux dissipation of high-power density devices. The importance of MCHS come also from its wide applications in thermal management of

* Corresponding author: mosab.sakkay@outlook.fr

batteries [2], CPUs, and GPUs [3]. One of the prominent techniques, in the cooling enhancement of the heat source is the integration of micro-structures, contributing to fluid mixing, and disruption of boundary layers. Thorough review had been conducted by Bhandari et al. [4] analyzing the effect of micro-structure of different geometries previously investigated and demonstrated their effectiveness [5]. Conclusions of their work highlighted passive strategies as eminent techniques in cooling micro-electronics.

According to Han et al. [6], repetitive disruption of dynamic and thermal boundary layers is the key factor for convective heat transfer enhancements. Profiled micro-structures demonstrated on their superiority in terms of thermohydraulic performance in the paper reported by Polat et al. [7]. In their work, numerical results showed that diamond micro-pillars' thermal performance overwhelmed that of square micro-pillars. A and Chakraborty [8] investigated the integration of pillars and holes into the MCHS with the purpose of finding the optimum combination, thus highest thermal and hydraulic performance. Owing to their work, elliptical micro-pin-fins demonstrated better thermohydraulic performance and low source temperature. Gao et al. [9] investigated through fluid flow characteristics and temperature distribution, the response of different arrangements of micro pin-fin arrays. Analyzing fluid flow characteristics showed that holes in-between rectangular fins result in enhancing fluid mixing. Helicoidal finned micro-pillars has improved fluid mixing and convective heat transfer via spanwise secondary flows [10]. Thus, inducing secondary flows contributes to improving thermal performance of the cooling system.

Owing to Song et al. [11], experimental and numerical work supplies initial population for optimization algorithms to resolve the multi-objective optimization issue of MCHS. Genetic Algorithm and Topology Optimization Algorithm have been employed recently to find compromise between contradictory objectives. As reported by Ismail et al. [12], multi-objective optimization coupled with artificial neural networks (ANNs) was applied to optimize the geometrical parameters of square-tapered micro-structures. In addition, Nekahi et al. [13] optimized fin shapes based on multi-objective optimization.

In a preceding work [14], performance of micro-structures in the shape of cylindrical pillars has been investigated and correlated with operating conditions. Extensive flow behavior has been analyzed and reported in this paper, clarifying the reasons behind cooling performance. Even though the scientific insights reported in this paper, configuration of cylindrical pillars have been producing only spanwise secondary flow with total remissness of normalwise secondary flow. As presented in several review works, researchers have been exploring micro-structures of different shapes and dimensions, and to the best of our knowledge, no consideration of horizontal micro-structures has been reported in prior works. Additionally, authors of the present manuscript suggest that horizontal micro-structures come up with normalwise secondary flow contributing to MCHS performance enhancement.

The current research focuses on exploring the novel configuration of micro-structures and the implementation pattern. Entropy generation has been considered as a key factor evaluating thermodynamic performance of the energy system. Furthermore, as thermal entropy generation and frictional entropy generation rates are contradictory and the purpose is to minimize them both, a preliminary Multi-Objective Optimization study has been conducted to provide Pareto front optimal solutions. The present paper reports a subset of extended numerical work, filling the gap of the unexamined horizontal micro-structures, with the purpose of upgrading thermal management of microelectronic components.

2 Problem statement

In the present section, the numerical methodology is described from physical model, mathematical model and numerical model perspectives.

2.1 Physical model

The MCHS under consideration consists of 62 parallel, straight microchannels with widths and heights of 205 µm and 404 µm, respectively. The MCHS removes heat from microelectronic components (CPU) as illustrated in fig. 1 and is covered by glass cover. Owing to the geometrical symmetry, only one channel, of 25mm length, has been conceived with a 10 mm of equal-distance repetitive micro-structures. Distance between two consecutive stations has been set to 200 µm, where each station contains either horizontal or vertical cylindrical pillar of 76 µm diameter (3/8 of the channel width [14]).

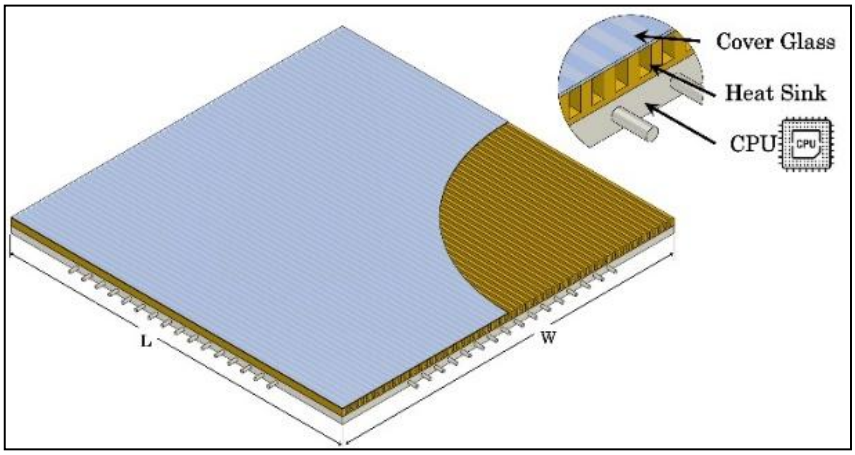

Fig. 1. Schematic view of the MCHS.

Tab. 1 represents the dimensions of the rectangular micro-channel, where subscripts MC and Ch stand respectively for the whole micro-channel heat sink domain and the flow region domain.

Table 1. Geometric dimensions.

Parameter	L	W	H_{MC}	W_{MC}	H_{Ch}	W_{Ch}
Dimension (μm)	25000	25000	501.5	400	404	205

2.2 Mathematical model

The conjugate heat transfer is studied under the following assumptions: three-dimensional steady state fluid flow, temperature-dependent fluid properties, and turbulent fluid flow considered in the effect of flow turbulators. Accounting for the previously established assumptions hypotheses, the governing equations are presented as:

Mass conservation equation

$$\nabla . (\rho_f \mathbf{V}) = 0 \quad (1)$$

where ρ_f and $\mathbf{V}$ represents the material density and the velocity.

Momentum conservation equation

$$\nabla . (\rho_f \mathbf{V}\,\mathbf{V}) = -\nabla p + \nabla . (\mu_f \mathbf{V}) \quad (2)$$

where μ_f and p are the material viscosity and the pressure.

Energy conservation equation

$$\nabla . (\rho_f C_{p,f} \mathbf{V} T) = \nabla . (k_f \nabla T) \quad (3)$$

$$\nabla.(k_s \nabla T) = 0 \quad (4)$$

where $C_{p,f}$, k_f, k_s, and T represents the material specific heat, fluid conductivity, solid conductivity, and the temperature.

2.3 Numerical model

The current paper's findings have been obtained through geometry construction under Autodesk Inventor Software, meshing under ANSYS MESH, and simulating leveraging ANSYS Fluent.

2.3.1 Computational Procedure

Based on FVM Method, Pressure and Velocity has been coupled using SIMPLE scheme and the governing equations are discretised using second order discretization with convergence criterion set to 10^{-6}.

2.3.2 Mesh Sensitivity Test

For the purpose of choosing the optimal mesh size and ensuring the independency of numerical results on meshing process, three grids of incremental size (element numbers) has been studied in this section. As Table 2 portrays, performance of the classical configuration (HP-MCHS) varies with the grid size. However, it is obvious that as size increases from 4.5 million element to 7.7 million element, *Nu* and *f* variation does not exceed 0.5%. Meaning that numerical results does not depend anymore on the mesh construction.

Table 2. Mesh sensitivity test.

Size	*Nu*	*f*
Number of elements [$\times 10^6$]	[−]	[−]
1.6	10.76	0.154
4.5	10.97	0.156
1.6	10.98	0.157

2.3.3 Model Validation

Present numerical results for conventional case (absence of mico-structures) has been compared to the data from experiments of Sui et al. [15] and found maximum relative deviation of 5.8% and 15.3%, respectively, in the prediction of heat transfer and fluid flow. Knowing that the max deviation falls within the uncertainty of the experimental results, one can say that no gap between numerical and experimental investigations has been found for the conventional micro-channel heat sink.

3 Results and discussion

Comparison of horizontal and vertical micro-structures embedded into micro-channel heat sink has been conducted, in the present section, considering entropy generation rate. Entropy

generation in the heat sink is created due to friction, as well as heat transfer, reflecting the irreversible nature of heat dissipation in MCHS. Thermal, frictional and total entropy production are evaluates using the following expressions.

$$S_{g,h} = q_h \cdot A_h \cdot (T_{int} - T_{f,in}) / (T_{int} \cdot T_{f,in}) \quad (5)$$

$$S_{g,f} = \Delta P \, (U_{f,in} \cdot A_c) / T_{f,in} \quad (6)$$

$$S_{g,tot} = q_h \cdot A_h \cdot (T_{int} - T_{f,in}) / (T_{int} \cdot T_{f,in}) + \Delta P \, (U_{f,in} \cdot A_c) / T_{f,in} \quad (7)$$

3.1 Thermodynamic Performance

3.1.1 Thermal entropy generation

The following figure (Fig. 2) illustrates the entropy production rate due to heat transfer. As Reynolds number increases, entropy production rate decreases for all configurations, owing to the higher convective heat transfer coefficients in large Reynolds number cases. Also, all tested configurations present an enhancement in terms of thermal entropy generation in comparison to conventional MCHS in all Reynolds number range.

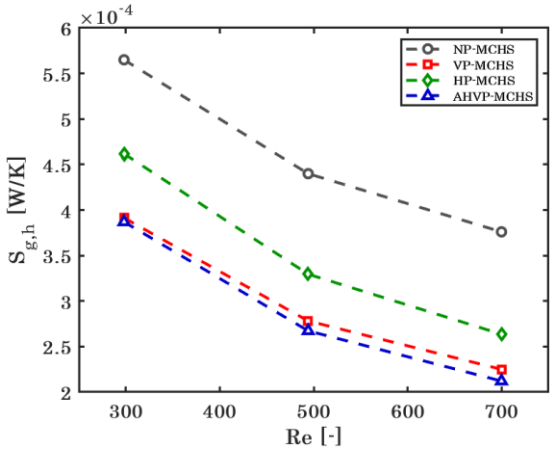

Fig. 2. Evaluation of thermal entropy generation rates.

3.1.2 Frictional entropy generation

Fig. 3 depicts the entropy production rate resulting from friction. One can say that production rate of frictional entropy increases as Reynolds number increases, owing to the higher flow resistance in the high flow velocities compared to that in the low flow velocities. Moreover, entropy production rate is higher in configurations with embedded micro-structures than in configurations with absence of micro-structures.

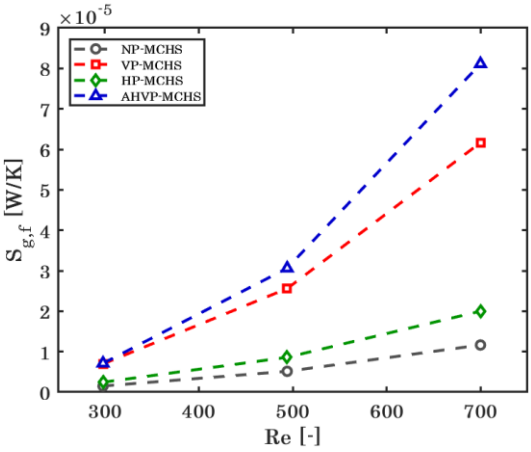

Fig. 3. Evaluation of frictional entropy generation rates.

3.1.3 Total entropy generation

As portrayed in fig. 4, total entropy production rate has been plotted versus Reynolds number for the various examined configurations. One can say, after analysing curve trends, that contradictory effects of micro-structure insertion on entropy production rates are mixed into total entropy generation. Effect of micro-structures insertion on diminishing thermal entropy generation overwhelms their effect on incremental frictional entropy generation. Conventional MCHS owns the highest entropy production rates among all presented configurations. Moreover, VP configuration demonstrates lowest entropy production at low Reynolds numbers while HP configuration demonstrates lowest entropy production at high Reynolds numbers.

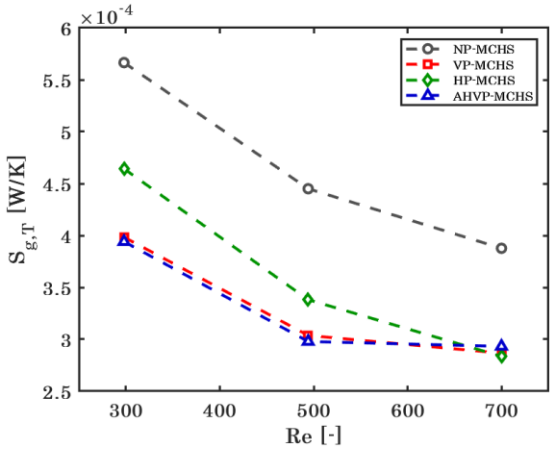

Fig. 4. Evaluation of total entropy generation rates.

3.2 Fluid flow and temperature field characteristics

3.2.1 Fluid flow

Fig. 5 portrays velocity distribution for the investigated micro-structures at highest Reynolds number. Contours, plot for an XY-plane at z = 0 µm, demonstrates that velocity in the entry region starts from a constant value and develops until having maximum velocity in the centre and zero-velocity near the walls. Moreover, in the exit region, flow in the downstream of micro-structures develops until no change occurs in the streamwise direction. From the distribution of the flow field, consecutive vertical pillars result in vortex zone all over the integration length of micro-structures (7.5 mm<x<17.5 mm). Furthermore, consecutive horizontal pillars result also in a vortex zone (7.5 mm<x<17.5 mm). One can say that, spacing between consecutive pillars is lower than vortex length. The present issue is a weakening problem where integration of micro-structures is limited by the constraint of vortex dimensions. In contrast to flow distribution for VP-MCHS and HP-MCHS, configuration AHVP-MCHS presents a better velocity profile based on the fact that two-consecutive vertical pillars and two-consecutive horizontal pillars are separated by larger distance, and thus bigger than vortex length. In other words, even though flow has not been developed in the downstream of a micro-structure, flow is disrupted with an opposite orientation micro-structure resulting in higher fluid mixing and contributing to re-establishment of fluid.

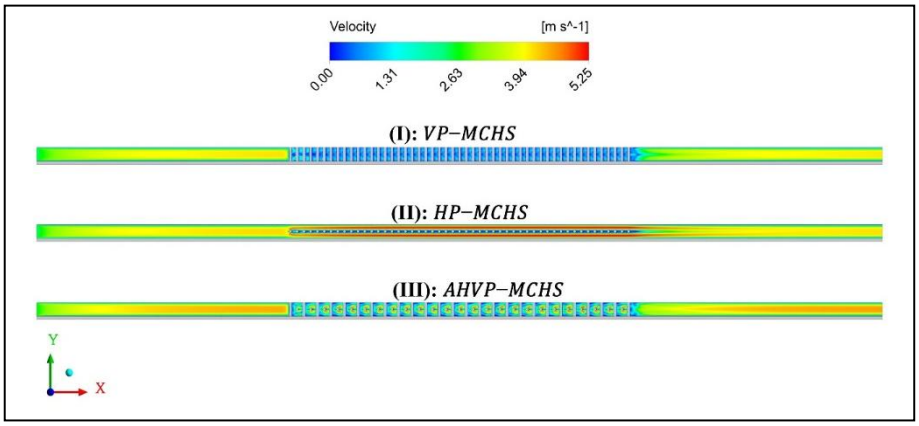

Fig. 5. Distribution of velocity field at plane XY, z = 0 µm.

3.2.2 Temperature field

Temperature contours have been plotted, similarly to previous analysis (Fluid flow characteristics), for plane XY at z=0 µm. Temperature distribution for the three investigated configurations demonstrates that AHVP-MCHS results in the best temperature uniformity due to mixed spanwise and normalwise secondar flow.

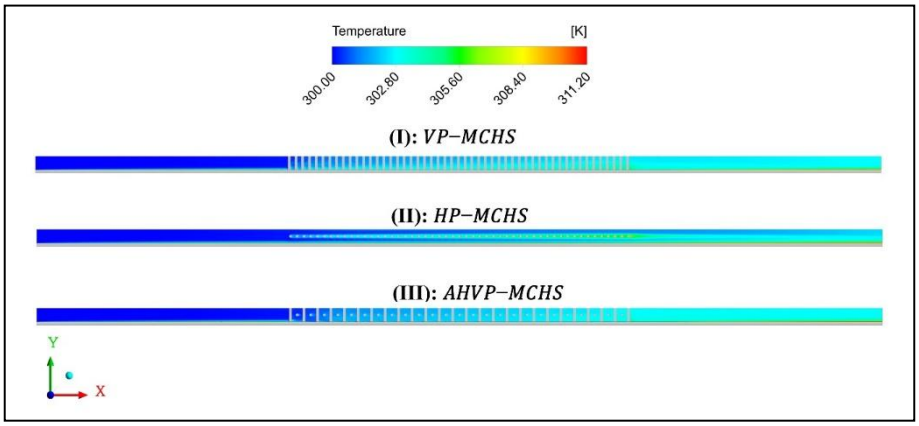

Fig. 6. Distribution of temperature field at plane XY, z = 0 μm.

4 Multi-Objective Optimization

As well-established in previous sections, several objectives are to be optimized simultaneously, considering their contradictory nature. The OV@T technique, that has widely been used in experimental and numerical experiences in order to investigate the effect of a single variable on response of the system, is not any more effective technique for optimizing configurations while variables have contradictory effect on MCHS performance. The present work considers Non-dominated Sorting Genetic Algorithm – II (NSGA-II) as multi-objective genetic algorithm, which finds optimal solutions of the Pareto front.

4.1 Objective functions

As studied in the present paper, entropy generation is the key parameter to evaluate thermodynamic performance of an energy system. While enhancement of thermal entropy production is usually accompanied with a diminishment of frictional entropy generation, they both should be considered as objective functions. Moreover, as total entropy generation is an addition of both thermal and frictional entropy generation rates, it is by default optimized when optimizing frictional and thermal entropy production rates.

$$OBJ_1 = S_{g,h} \tag{8}$$

$$OBJ_2 = S_{g,f} \tag{9}$$

4.2 Independent variables

The present paper investigates the effect of micro-structure's pattern on thermodynamic performance of MCHS. Furthermore, Reynolds number has also an important effect on the system's performance. For this reason, these two independent variables has been considered for the multi-objective optimization study in the present paper.

4.3 Pareto front

Fig. 7 illustrates the non-dominated solutions of the two-objective optimization Pareto front distribution. A comprehensive trade-off between the two optimized objective functions has been found and presented where there is no superiority between the solutions. Minimum solutions in terms of $S_{g,f}$ and $S_{g,h}$ are marked, respectively, with red and green colors.

Moreover, optimal solution in terms of thermal entropy generation has been obtained for AHVP pattern for highest Reynolds number. Pareto front solutions, as illustrated in this figure, contain multiple solutions offering compromise between the two-objectives where ideal optimal solution is the closer to the ends of the Pareto front. Thus, it is necessary to employ a decision-making algorithm to select the ideal optimal solution from the Pareto front.

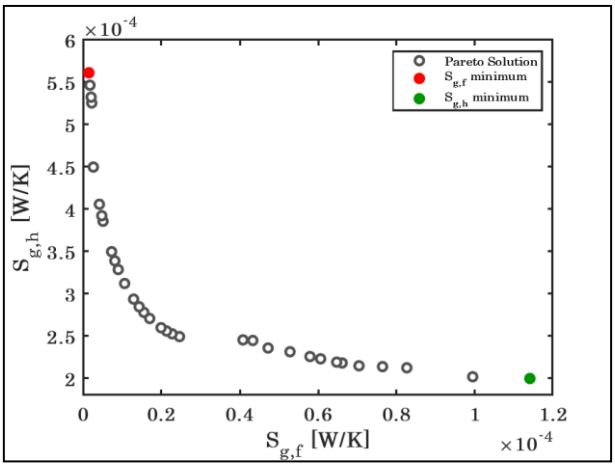

Fig. 7. Optimized Pareto front distribution.

5 Conclusion

In the present conference paper, a preliminary investigation of horizontal micro-structures has been conducted through entropy generation analysis. Effect of micro-structure's integration pattern has been evaluated for 4 patterns and 3 Reynolds numbers. Fluid flow distribution has been presented and discussed to optimize the vortex generators from a point of view of fluid mixing. Temperature contours have been analysed to understand effect of micro-structure's pattern on thermal boundary layer on fin walls as well as on pillar's walls. The results have demonstrated that, alternating micro-structures of horizontal and vertical orientations, leads to the best thermodynamic performance, as a result of enhanced spanwise and normalwise secondary flow.

This work presents a subset of the findings from a broader work in progress. Additional micro-structure's integration patterns are currently under investigation to evaluate cooling performance for other patterns. Moreover, future work considers thermal and thermohydraulic performance where the present work is limited to thermodynamic performance evaluation. Also, local mesh sensitivity test with the use of polyhedral mesh elements would be an important step towards credibility of numerical results. In addition, ANOVA test will be conducted to determine interaction of independent variables, followed by ANN fitting and multi-objective optimization of three objective functions and more independent variables. As well, decision-making algorithm will be employed to select ideal optimal solution. Extended results, under larger Reynolds numbers, considering non-dimensional structural parameters, will be analysed extensively and published in forthcoming work.

Nomenclature

General symbols & Abbreviations	
ANOVA	Analysis of Variance
ANN	Artificial Neural Network
AHVP-MCHS	Alternated Horizontal and Vertical Pillars integrated into MCHS
CFD	Computational Fluid Dynamics
CPU	Central Processor Unit
FVM	Finite Volume Method
HP-MCHS	Horizontal Pillars integrated into MCHS
MCHS	Micro-Channel Heat Sink
MOO	Multi-Objective Optimization
OV@T	One Variable At Time
UDF	User Defined Functions
VP-MCHS	Vertical Pillars integrated into MCHS
Greek symbols	
ρ	Density ($kg.m^{-3}$)
μ	Dynamic viscosity ($kg.m^{-1}.s^{-1}$)
Subscripts & superscripts	
Ch	Channel flow region
f	Fluid
h	Heated surface
in	Fluid inlet
int	Fluid/ Solid Interface
MC	Total Micro-Channel region
t	Turbulent

References

1. D. B. Tuckerman, R. F. W. Pease, Z. Guo, J. E. Hu, O. Yildirim, G. Deane, L. Wood, in Microchannel Heat Transfer: Early History, Commercial Applications, and Emerging Opportunities, *ICNMM2011* (ASME 2011 9th International Conference on Nanochannels, Microchannels, and Minichannels, Volume 2, 2011), pp. 739–756
2. L. Huang, T. Yuan, Y. Wang, H. Guo, X. Guo, X. Li, B. Chang, Y. Wang, X. Xi, Numerical Investigation and Optimization on Thermal Management of a DC-Bus Film Capacitor in Electric Vehicle Using Microchannel Cooling Plates, Appl. Therm. Eng. **244**, 122695 (2024)
3. X.-H. Yang, S.-C. Tan, Y.-J. Ding, J. Liu, Flow and Thermal Modeling and Optimization of Micro/Mini-Channel Heat Sink, Appl. Therm. Eng. **117**, 289 (2017)
4. P. Bhandari, K. S. Rawat, Y. K. Prajapati, D. Padalia, L. Ranakoti, T. Singh, A Review on Design Alteration in Microchannel Heat Sink for Augmented Thermohydraulic Performance, Ain Shams Eng. J. **15**, 102417 (2024)
5. J. Tang, A Novel Designed Manifold Ultrathin Micro Pin-Fin Channel for Thermal Management of High-Concentrator Photovoltaic System, Int. J. Heat Mass Transf. **183**, 122094 (2022)
6. Q. Han, Z. Liu, W. Li, Enhanced Thermal Performance by Spatial Chaotic Mixing in a Saw-like Microchannel, Int. J. Therm. Sci. **186**, 108148 (2023)
7. M. E. Polat, F. Ulger, S. Cadirci, Multi-Objective Optimization and Performance Assessment of Microchannel Heat Sinks with Micro Pin-Fins, Int. J. Therm. Sci. **174**, 107432 (2022)

8. R. A, S. Chakraborty, Effect of Shape and Arrangement of Micro-Structures in a Microchannel Heat Sink on the Thermo-Hydraulic Performance, Appl. Therm. Eng. **190**, 116755 (2021)
9. J. Gao, Z. Hu, Q. Yang, X. Liang, H. Wu, Fluid Flow and Heat Transfer in Microchannel Heat Sinks: Modelling Review and Recent Progress, Therm. Sci. Eng. Prog. **29**, 101203 (2022)
10. M. Sakkay, I. El Ghandouri, A. El Maakoul, S. Saadeddine, M. Meziane, A. Dani, Advanced Thermal Management of High-Power Density Devices: Helicoidally Finned Micro-Pillars in Microchannel Heat Sinks, Case Stud. Therm. Eng. **75**, 107098 (2025)
11. G. Song, H. Chen, Y. Zhang, J. Wei, X. Ma, Reviews: Applications of Optimization Algorithm for Microchannel and Microchannel Heat Sink on Heat Transfer, Int. J. Heat Fluid Flow **108**, 109451 (2024)
12. O. A. Ismail, A. M. Ali, M. A. Hassan, O. Gamea, Geometric Optimization of Pin Fins for Enhanced Cooling in a Microchannel Heat Sink, Int. J. Therm. Sci. **190**, 108321 (2023)
13. S. Nekahi, F. Sadegh Moghanlou, K. Vaferi, H. Ghaebi, M. Vajdi, H. Nami, Optimizing Finned-Microchannel Heat Sink Design for Enhanced Overall Performance by Three Different Approaches: Numerical Simulation, Artificial Neural Network, and Multi-Objective Optimization, Appl. Therm. Eng. **245**, 122835 (2024)
14. M. Sakkay, I. EL Ghandouri, A. EL Maakoul, S. Saadeddine, M. Meziane, A. Dani, Enhancing Heat Transfer Efficiency and Entropy Generation Minimization in Micro-Channel Heat Sinks through Pillar Spacing and Diameter Optimization, Int. J. Heat Fluid Flow **108**, 109492 (2024)
15. Y. Sui, P. S. Lee, C. J. Teo, An Experimental Study of Flow Friction and Heat Transfer in Wavy Microchannels with Rectangular Cross Section, Int. J. Therm. Sci. **50**, 2473 (2011)